Integrating activated sludge floc size information in MBR fouling modeling

T. A. Cao, G. Van De Staey and I. Y. Smets

ABSTRACT

Although studied extensively, modeling fouling phenomena in membrane bioreactors (MBRs) remains challenging. It has been well established that cake layer formation and pore blocking have a strong impact on the filtration performance but how to capture that in comprehensive models is not fully defined yet. Since it has been shown that bioflocculation characteristics of activated sludge have a clear link with (the extent of) membrane fouling, this study integrates activated sludge floc size (i.e., particle size distribution) information in the model for pore blocking and cake layer formation with a focus on constant flux operated MBRs. Based on these floc size distributions, a three-dimensional modeling and visualization of the cake layer is envisaged which can then provide the required input information (e.g., the porosity of the cake layer) for the fouling model. The model is calibrated and validated on the basis of experimental data from Hwang *et al*. (2012) in 'Membrane bioreactor: TMP rise and characterization of biocake structure using CLSM-image analysis' (see *J. Membr. Sci.* 419–420, 33–41).

Key words | activated sludge, cake layer, MBR fouling, modeling, particle size distribution

T. A. Cao
G. Van De Staey
I. Y. Smets (corresponding author)
Chemical Engineering Department,
KU Leuven, BioTeC - Chemical and Biochemical Process Technology and Control,
W. de Croylaan 46,
B-3001 Leuven, Belgium
E-mail: *ilse.smets@cit.kuleuven.be*

INTRODUCTION

Over the last decades, membrane bioreactors (MBRs) have proven to be a promising technology in the field of wastewater treatment. However, the major bottleneck for the technology, which significantly increases the overall operation cost, remains membrane fouling. During the operation of an MBR, a layer of retained particles deposits on the membrane surface to form a cake layer of which the structure and thickness determine the degree of membrane fouling. Therefore, it is important to understand the mechanism of this cake layer formation and to be able to link this cake layer formation to directly measurable characteristics of the mixed liquor in the MBR such as particle size distributions (PSDs) of the activated sludge. It has, indeed, been shown in many studies that bioflocculation (which will determine the fraction of submicron particles in the PSD) has a strong impact on MBR fouling (Bouhabila *et al*. 1998; Wisniewski *et al*. 2000; Le-Clech *et al*. 2006; Ivanovic *et al*. 2008; Van den Broeck *et al*. 2010; De Temmerman *et al*. 2014; Faust *et al*. 2014).

There are many different approaches to model cake layer formation in MBRs. We focus in the following literature review on those contributions that take particles into account for a structural cake layer build-up and/or predict, apart from the thickness, also the porosity of the cake layer. Lu & Hwang (1993) propose the concept of a critical friction angle between particles for studying cake layer formation for constant pressure filtrations. By taking a force balance on a depositing particle, the value of the critical friction angle is determined and the structure of the cake is simulated numerically. Shin *et al*. (2013) approach cake layer formation through a lattice Bolzmann method by integrating the hydrodynamics of the system. The model is able to simulate the cake layer structure in three dimensions (3D) and to examine the influence of a specific (unique) particle size on the cake layer thickness. They, however, also work in a constant pressure mode (whereas most MBRs are operated in constant flux mode) and cannot take into account a PSD. Park *et al*. (2006) developed a model based on fractal theory and incorporated a cake collapse effect to predict the porosity and permeability of the cake layers. The porosity in the cake is estimated as a function of floc size, fractal dimension and transmembrane pressure, but in a dead-end filtration setting which is not representative of classic MBR filtrations in which air scouring is present. A sectional method is employed by Li & Wang (2006) to account for the non-uniform distributions of both the turbulence intensity and fouling material coverage on the membrane surface, but the required model inputs and parameters cannot

doi: 10.2166/wst.2015.070

directly be inferred from mixed liquor characteristics (and no porosity of the cake layer is predicted). Picioreanu *et al.* (2004) introduce a spatially multidimensional (2D and 3D) particle-based approach for modeling the dynamics of multispecies biofilms growing on multiple substrates. The model is based on diffusion-reaction mass balances for chemical species coupled with microbial growth and spreading of biomass represented by hard spherical particles. Although this biofilm formation is important in explaining the filtration performance degradation over time, this model does not cover the (removable) cake layer that is built up during the filtration phase itself. Three-dimensional simulations of rigid spherical particles are discussed by Yoon *et al.* (1999) to predict the flux during the microfiltration. A time curve of the flux decline is obtained by considering the cake resistance from the random packing of unequal sized particles as well as the pore blocking resistance. Finally, the model which is proposed by Broeckmann *et al.* (2006) takes into account the influence of particle and membrane pore size distributions on both cake layer formation and pore blocking and their mutual dependencies.

With an overall aim to link the PSD of the activated sludge in the mixed liquor and the overall operational condition to the (3D) structural build-up of the cake layer during filtration and relaxation of a common 'constant flux' operated MBR, it was decided to explore the integration of floc (particle) size distribution information in the model proposed by Broeckmann *et al.* (2006) and impose particle deposition rules inspired by the approach of Yoon *et al.* (1999).

THEORY

In the following we first provide a summary of the overall algorithm and then explain the different steps in somewhat more detail.

Overall algorithm

The cake layer is formed at one side of the membrane by a fraction of the bulk particles that is able to deposit on the membrane surface. The flowchart of the model is shown in Figure 1 and is briefly described in the following.

- The PSD of the activated sludge is inferred. In our case, this is done on the basis of the in-house developed image analysis tool ACTIAS (Jenné *et al.* 2002, 2007).

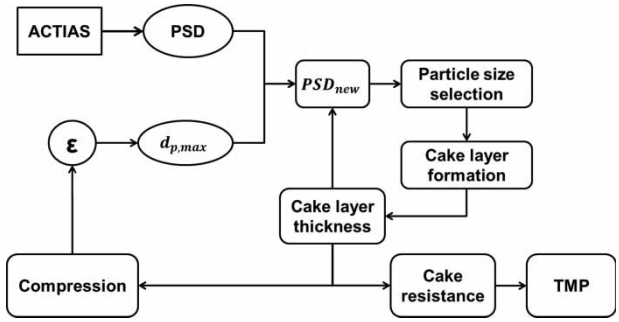

Figure 1 | Overall modeling flow.

- Based on the Broeckmann model, the value of the cut-off diameter ($d_{p,\max}$) is calculated. Particles which have sizes smaller than $d_{p,\max}$ are able to deposit and constitute together a new PSD. Broeckmann's model exploits a balance of forces around the particle (with diameter d_p) and the Blake–Kozeny equation to describe the fluid dynamics to yield a dynamic model for the cake layer formation and resistance (Broeckmann *et al.* 2006). In view of size limitations, only the final expression of $d_{p,\max}$ is mentioned here.

$$d_p \leq \frac{\mu_{\max}.k_s.\eta.J}{\tau^W}.\left(360.k_{\text{kozeny}}.\frac{(1-\varepsilon)^2}{\varepsilon^3}\right)^{0.4} = d_{p,\max} \qquad (1)$$

- The cake layer is built up by depositing different particles (which are assumed to be spherical) from this new distribution (delimited by $d_{p,\max}$). Cake layer build-up is stopped when the total amount of biomass that can deposit on the membrane during one filtration cycle is reached.
- Compression is applied to the cake layer at the end of each filtration/backwash cycle. From this (compressed) layer, the cake layer porosity is calculated and used to calculate the cut-off diameter ($d_{p,\max}$) for the next cycle together with the cake layer resistance, the transmembrane pressure (TMP) and the cake layer thickness.

Simulation of the membrane surface

The membrane surface is a simulated area with size of 60 μm by 60 μm. All pores have the same diameter of 0.4 μm and the pore density is 10^{12} per m^2 in each simulation, mimicking a commercial microfiltration membrane. The pores are assumed to be circular in shape. Based on the empirical pore density, the distance between the centers of two adjacent pores is 1 μm.

Deposited particle size distribution and particle size selection

The particles which have sizes smaller than $d_{p,\max}$ (Equation (1)) are able to deposit on the membrane surface. Therefore, from the original PSD of the bulk activated sludge flocs, a new PSD is inferred, delimited by the $d_{p,\max}$ value. All the particles which are able to deposit on the membrane surface have the same probability of being selected. Therefore, the probability of selecting a particle from a certain size class from this new distribution is proportional to the relative abundance of the corresponding size class. Note that the $d_{p,\max}$ value is calculated at the beginning of each cycle and tends to increase in time because of the reducing porosity. Hence, subsequent PSDs include bigger and bigger particles.

In this study, in order to validate and calibrate the model on the basis of the data of Hwang *et al.* (2012), a PSD is manually created using the normally distributed pseudorandom number function (randn – MatLab) to mimic a distribution centered around the given average particle size of 160 μm.

Particle depositing rules

The depositing rules of a particle are basically developed from the particle packing rules described by Yoon *et al.* (1999). The particles, assumed to be spheres, are deposited one by one onto the membrane surface so as not to overlap each other. The first location of the depositing particle is generated randomly within the area of the simulated membrane surface. The particle will keep dropping until it reaches the membrane surface or touches a previously deposited particle. In case the particle does not touch any deposited particle, it will stay on the membrane surface, and it is tested whether it blocks some pores or not according to the blocking condition described in the next section. If the depositing particle is able to touch one particle, it will take that touchable particle as the first contacting particle and will roll down, over the surface of that particle. If the depositing particle is going to touch more than one particle (checked by looking at a projection of the falling particle on the membrane/cake layer surface), it needs to be defined which particle in the set of touchable particles is the first contacting particle. The particle which has to be defined as the first contacting particle is the one which yields the highest z-position to the depositing particle. The rolling direction of the depositing particle (after having touched the first particle) is driven by the direction of the projection of the vector drawn from the center of the contacting particle to the depositing particle on the $[x,y]$ horizontal plane.

During the rolling of the depositing particle, it may touch a second contacting particle. Then there are two possibilities for the movement of the depositing particle. One is that the depositing particle rolls around the two contacting particles. The vector which shows the moving direction of the depositing particle is calculated by summing two vectors from the center of the first and second contacting particles to the center of the depositing particle. It is different from the rolling algorithm proposed by Yoon *et al.* (1999) where the particle rolls again via the center line of both spheres. The depositing particle keeps rolling until either it touches a third particle or falls freely after the rolling process. The second possibility is that the depositing particle rolls around the first contacting particle, then touches the second contacting particle, after which it keeps rolling over the second contacting particle and detaches from the first contacting particle. The second contacting particle now behaves like a first contacting particle.

During rolling around two deposited particles, the depositing particle may touch the third contacting particle and will stay there, in balance with the three neighboring particles. If not, it will keep falling and ends up at the membrane.

A 3D cake layer model is successfully built based on these particle packing rules and a resulting 3D cake layer is illustrated in Figure 2.

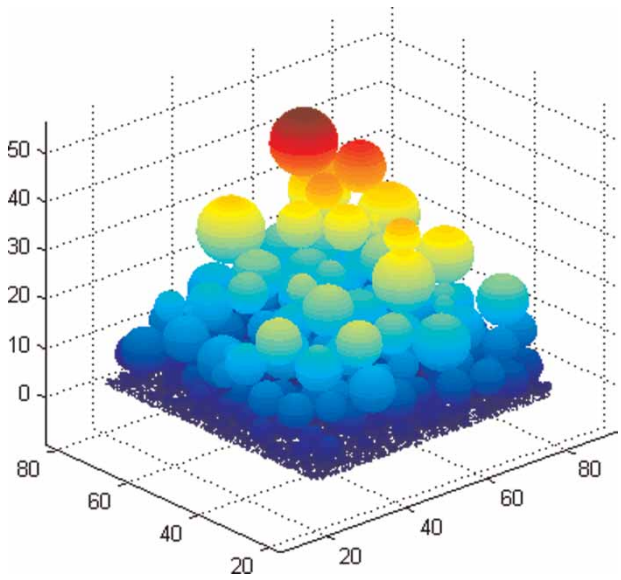

Figure 2 | 3D cake layer with multi-size particles after filtration.

Blocking condition

Pores are considered to be blocked by particles touching the membrane surface and covering the whole pore area. If a particle is considered to block a pore but its size is smaller than the pore size, it will go through the pore and the pore remains unblocked. After pores get blocked, particles will not be able to deposit on those areas but they can be diverted to it due to rolling movements.

Transmembrane pressure calculation

The transmembrane pressure of the membrane is described by the Darcy equation

$$\Delta P = J_{\text{eff}}.R_{\text{total}}.\eta \tag{2}$$

The overall resistance R_{total} is modeled using the conventional resistances-in-series approach, including the membrane resistance R_{mem} and the combined cake layer/blocking resistance (R_{cake})

$$R_{\text{total}} = R_{\text{mem}} + R_{\text{cake}} \tag{3}$$

The membrane resistance R_{mem} value is experimentally determined and the cake layer resistance R_{cake} is the sum of the resistances of all the sublayers in the deposited cake as described in Equation (4)

$$R_{\text{cake}} = \sum_{i=1}^{\text{number of sublayer}} L_{\text{sublayer},i}.K_{\text{sublayer},i} \tag{4}$$

The cake layer thickness is the same for all the sublayers within the deposited cake layer. The specific sublayer resistance is again calculated by using the Blake–Kozeny equation (Equation (5))

$$K_{\text{sublayer},i} = \frac{k_{\text{kozeny}}.90}{\overline{d_p^2}}.\frac{(1-\varepsilon_{\text{sublayer},i})^2}{\varepsilon^3_{\text{sublayer},i}} \tag{5}$$

The calculation of the porosity of sublayer-ith ($\varepsilon_{\text{sublayer},i}$) will be described in the next section.

The effective flux J_{eff} is calculated by taking into account the ratio of the total number of membrane pores, N_0, to the remaining unblocked pores after each cycle, N.

$$J_{\text{eff}} = J.\frac{N_0}{N} \tag{6}$$

Porosity calculation and compression

The cake layer porosity is calculated at the end of each filtration cycle but once a certain cake layer has been built up, one can calculate a porosity profile by plotting a series of sublayer porosities along the cake depth with a certain sublayer thickness (here specified as 1 μm). The (parts of) particles that lie within a certain sublayer are used to calculate the porosity of that sublayer on the basis of Equations (7) and (8).

$$\varepsilon_{\text{sublayer},\,i} = 1 - \theta_i \tag{7}$$

θ_i: bacterial cells fraction in sublayer-ith
in which

$$\theta_i = \frac{\sum \text{Volume}_{\text{bacterial cells within sublayer},i}}{\text{compression\_factor}.\text{Volume}_{\text{sublayer},i}} \tag{8}$$

In addition, compression is applied to the gradually forming cake layer by using a compression factor which is smaller than 1. The volumes of the deposited particles from the previous cycles are kept constant but the volume of the by then built up cake in which these particles 'reside' is compressed by a factor. Note that this pragmatic way of implementing compression can also reflect the increase of the particle sizes (e.g., by extracellular polymeric substances (EPS) formation within biofilm-like patches of the cake layer).

RESULTS

Model calibration and validation

The model is calibrated and validated by using the experimental data reported in the work of Hwang *et al.* (2008, 2012). Three identical membrane modules (being polyethylene hollow fiber microfiltration membranes (KMS, Korea) with a nominal membrane pore diameter of 0.4 μm) were operated under constant fluxes of 13, 20 and 27 L/m^2·h, respectively, without backwash cycles. The continuous filtration was stopped when the TMP reached 30 kPa. The concentration of the mixed liquor suspended solids was maintained at 8.2 g MLSS/L in the membrane reactor. The temperature was maintained at 25 °C.

The volume fraction of bacterial cells and polysaccharides along the cake depth was obtained by using confocal laser scanning microscopy in combination with the image

structure analyzer software in 3D (ISA-2) (Hwang *et al.* 2012). From these data we calculated the total volume fraction of the occupied space by both bacterial cells and polysaccharides within the cake layer, which we need to validate the porosity profiles because the volume fraction of occupied space in the cake layer is 1 minus the porosity value.

The experimental data of the transmembrane pressure build-up during the filtration and the total volume fraction of bacterial cells and polysaccharides along the cake depth with a constant flux of 27 L/m^2·h are used for the model calibration. In the model calibration, the empirical parameters such as R_{mem}, k_s, k_{kozeny} and shear stress, τ^{av}, are kept constant, with values of 5.10^{11}, 1,886, 25 and 2, respectively. The compression factor is a calibrated value of 0.999. The data of the membrane filtration experiments with constant flux of 13 and 20 L/m^2·h are then used for model validation (Figure 3).

For a typical MBR filtration process, there is usually a period of slow TMP increase leading to a time instance after which a sharp, exponential increase (according to the critical flux concept; see, for example, Ognier *et al.* 2004) is observed. This typical profile is corroborated by the experimental and simulated data shown in Figure 3(a). Notice that the deviation of the initial TMP for the three different fluxes is due to the very limited effect of pore blocking that we encounter in this experiments due to a lack of full knowledge of the size distribution of the sludge.

Figure 3(b), 3(c) and 3(d) show the comparison of porosity profiles at different fluxes between the experimental and the simulated data. It can be seen that the porosity decreases until the cake layer thickness reaches 5–10 μm and starts increasing after that. By analyzing the contribution of different particle sizes to this cake layer thickness from 5 to 10 μm, it can be inferred that the

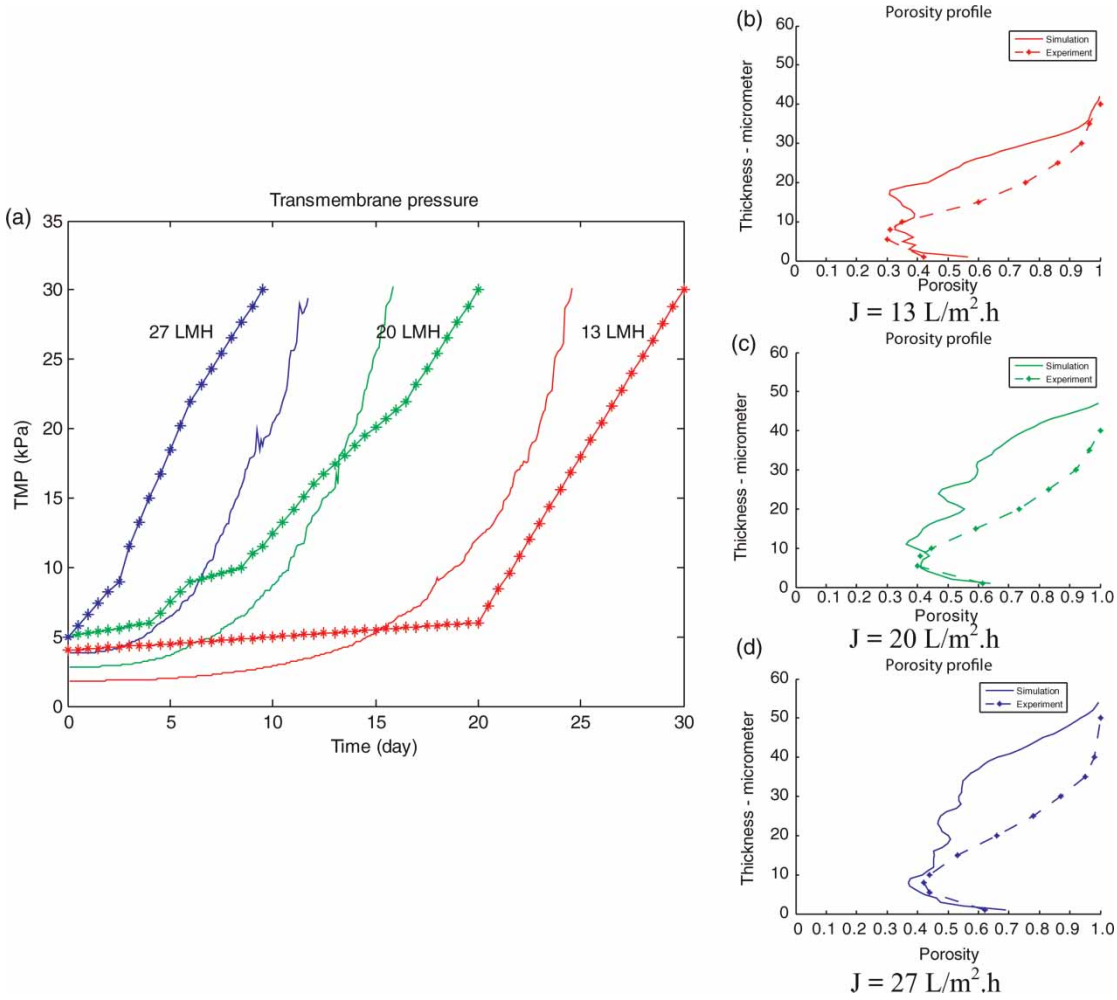

Figure 3 | Comparisons of the TMP and porosity profile between experimental and simulated data (*: experimental data, ——: simulated data).

majority of the particle sizes presents in this layer range from 0.5 to 5 μm. This small particle size range has, therefore, a strong impact on the reduction of the porosity. The impact of these small particles on membrane fouling was also observed in other MBR related research (Meng & Yang 2007; Van den Broeck *et al.* 2010). The simulated porosities in the bottom part of the cake layer agree very well with the experimental data. The simulated cake layer thickness and porosity in the upper layer (from 10 μm on) match less well with the experimental data, which is due to the lack of information on the real PSD and the use of the fixed calibrated compression factor. Note, furthermore, that the lowest porosity values are obtained in the cake built up under the lowest flux value. This can be explained by the fact that, at this flux, the maximum diameter of the particles that can be deposited ($d_{p,\max}$) is small, such that the relative abundance of the 0.5–5 μm particles is much higher at low fluxes, which results in a dense cake layer. The TMP jump occurs, however, later than at high fluxes given that the TMP has a direct relation with the flux value.

Influence of compression

Figure 4(a1) and 4(b1) show a strong influence of compression on the development of transmembrane pressure and porosity profile. For the cake layer without compression, it takes a longer time to reach the TMP of 30 kPa, i.e., 23 days instead of 11 days (Figure 4(a1)). The cake layer with compression has a lower porosity and is also thicker due to the contribution of bigger particles which are able to deposit with an increase in the cake resistance and the corresponding increasing $d_{p,\max}$ value (Figure 4(b1)). Cake layer compression is difficult to quantify but the trend observed here is in line with, for example, the results described by Bugge *et al.* (2012) and Jørgensen *et al.* (2012). The relation between the compression and the specific resistance and pressure, as described by the latter authors, will be explored in future research.

Influence of shear stress

Shear stress has been recognized as an important parameter to control membrane fouling: by applying a stronger shear stress, the time to reach TMP of 30 kPa is longer (Figure 4(a2)). With a reduced shear stress, the porosity of the cake layer decreases (Figure 4(b2)) and larger particles can be present in the cake, which increases the cake layer thickness. A higher shear stress is clearly more effective to reduce the membrane fouling, which corroborates the results of, for example, Choi *et al.* (2005) and Pradhan *et al.* (2014).

Influence of PSD

To determine the influence of PSD, a new PSD, PSD_2, has been designed in which the fraction of the particles with the sizes smaller than 1 μm is three times higher than in the original PSD_1. Increasing these smaller particle sizes results in a thicker cake layer of lower porosity (Figure 4(b3)), which leads to an increase of cake resistance as well as to a rapid increase of TMP. It takes about 8 days to reach TMP of 30 kPa instead of 11 days in the case of PSD_1 (Figure 4(a3)), again corroborating the impact of small particles on membrane fouling. A similar influence of small particles is also observed by, for example, Meng & Yang (2007), Van den Broeck *et al.* (2010), Faust *et al.* (2014) and De Temmerman *et al.* (2014). Shin *et al.* (2013) observe, however, a thicker cake layer when working with a larger (single) particle size, demonstrating the importance of working with a PSD to unravel the structural cake layer build-up.

As a final discussion point, it must be stressed that, to really fine-tune this type of modeling, data of the cake layer 'during' the filtration part itself are still missing. If cake layer thicknesses and porosities are reported, these are resulting from residual fouling on the membrane (once you take the membrane out of the system). But what of the cake layer build-up during the (e.g., 8 minutes) filtration part? Once you stop filtering to take the membrane out, this cake layer ceases to exist. In collaboration with others, the authors are working on a monitoring tool to have an idea of the *in-situ* filtration cake layer characteristics, which would be extremely valuable in further optimizing the model proposed here.

CONCLUSIONS

By combining the model proposed by Broeckmann *et al.* (2006) with activated sludge PSDs and particle deposition rules inspired by Yoon *et al.* (1999), a 3D cake layer with multi-size particles has been developed. A good agreement is obtained between experimental and simulated data. The model demonstrates the strong influence of PSD, compression and shear stress on the characteristics of the formed cake layer. The added value of the model is the fact that (i) a porosity profile along the cake thickness is predicted (and not just an average porosity), (ii) the impact (and location) of different particle sizes on the porosity and cake

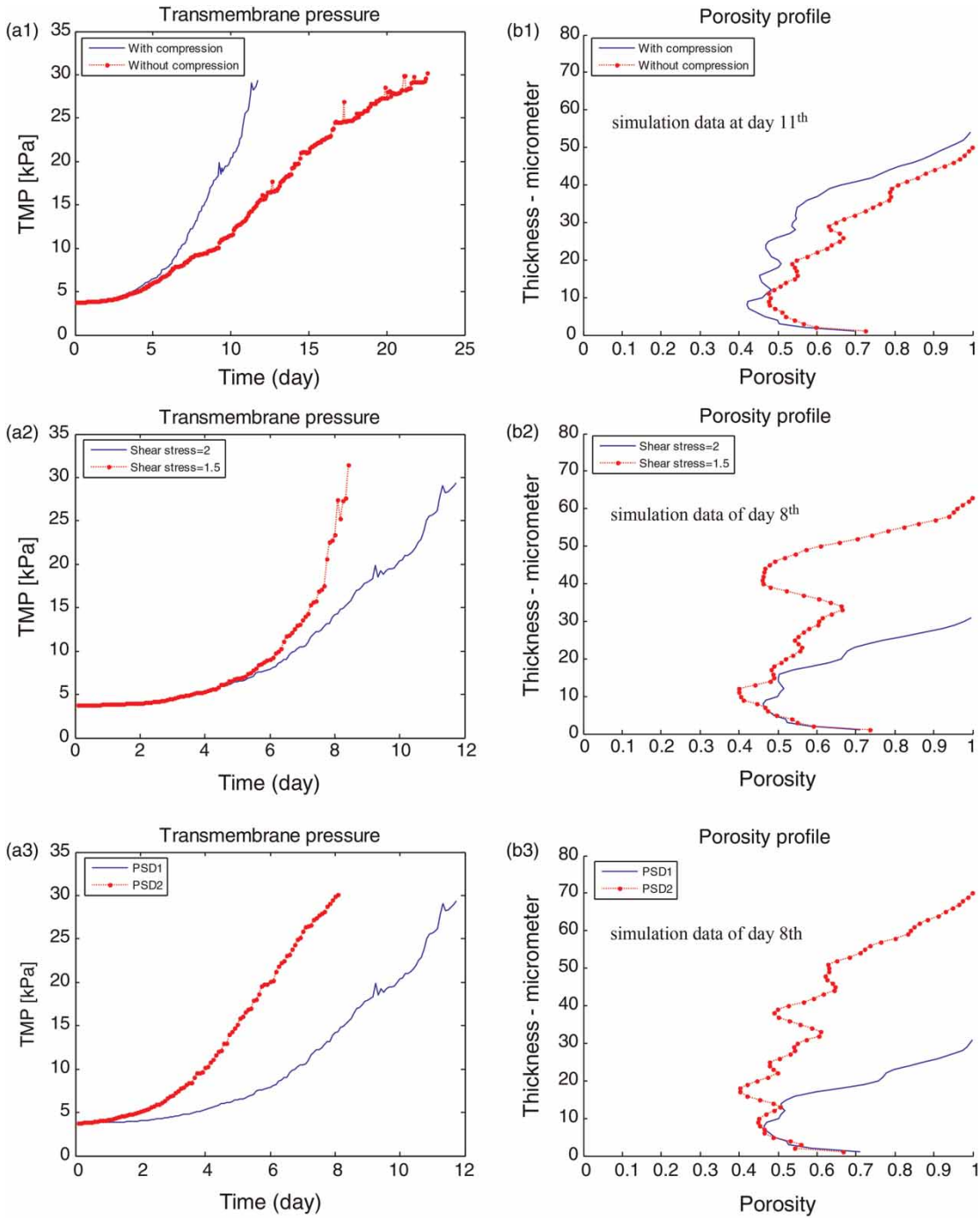

Figure 4 | Influence of compression, shear stress and PSD on (a) the TMP profile (b) the porosity profile at the flux of 27 L/m^2·h.

layer resistance can be inferred to enable a better understanding of the link between activated sludge (size) characteristics and membrane fouling, and (iii) pore blocking and compression are integrated. The model is, furthermore, suited to be linked to a hydrodynamic model to provide a more dynamic and realistic shear stress input to the model. The improvement in the expression of compression, more accurate PSD data and, if possible, *in-situ* cake layer characteristics during filtration will also help to significantly improve the model quality. Finally, in the long run, this model could be coupled to a biological model that predicts the bioflocculation state of the activated

sludge (induced by influent and operational characteristics) from which the required PSD evolves.

REFERENCES

Bouhabila, E. H., Ben Aim, R. & Buisson, H. 1998 Microfiltration of activated sludge using submerged membrane with air bubbling (application to wastewater treatment). *Desalination* **118** (1), 315–322.

Broeckmann, A., Busch, J., Wintgens, T. & Marquardt, W. 2006 Modeling of pore blocking and cake layer formation in membrane filtration for wastewater treatment. *Desalination* **189**, 97–109.

Bugge, T. V., Jørgensen, M. K., Christensen, M. L. & Keiding, K. 2012 Modeling cake buildup under TMP-step filtration in a membrane bioreactor: cake compressibility is significant. *Water Res.* **46**, 4330–4338.

Choi, H., Zhang, K., Dionysiou, D. D., Oerther, D. B. & Sorial, G. A. 2005 Influence of cross-flow velocity on membrane performance during filtration of biological suspension. *J. Membr. Sci.* **248**, 189–199.

De Temmerman, L., Maere, T., Temmink, H., Zwijnenburg, A. & Nopens, I. 2014 Salt stress in a membrane bioreactor: dynamics of sludge properties, membrane fouling and remediation through powdered activated carbon dosing. *Water Res.* **63**, 112–124.

Faust, L., Temmink, H., Zwijnenburg, A., Kemperman, A. & Rijnaarts, H. 2014 High loaded MBRs for organic matter recovery from sewage: effect of solids retention time on bioflocculation and on the role of extra-cellular polymers. *Water Res.* **56**, 258–266.

Hwang, B. K., Lee, W. N., Yeon, K. M., Park, P. K., Lee, C. H., Chang, I. S., Drews, I. S. A. & Kraume, M. 2008 Correlating TMP increase with microbial characteristics in the bio-cake on the membrane surface in a membrane bioreactor. *Environ. Sci. Technol.* **42**, 3963–3968.

Hwang, B. K., Lee, C. H., Chang, I. S., Drews, A. & Field, R. 2012 Membrane bioreactor: TMP rise and characterization of bio-cake structure using CLSM-image analysis. *J. Membr. Sci.* **419–420**, 33–41.

Ivanovic, I., Leiknes, T. & Odegaard, H. 2008 Fouling control by reduction of submicron particles in a BF-MBR with an integrated flocculation zone in the membrane reactor. *Sep. Sci. Technol.* **43** (7), 1871–1883.

Jenné, R., Cenens, C., Geeraerd, A. H. & Van Impe, J. F. 2002 Towards on-line quantification of flocs and filaments by image analysis. *Biotechnol. Lett.* **24**, 931–935.

Jenné, R., Banadda, E. N., Smets, I. Y., Deurinck, J. & Van Impe, J. F. 2007 Detection of filamentous bulking problems: developing an image analysis system for sludge composition monitoring. *Microsc. Microanal.* **13** (1), 36–41.

Jørgensen, M. K., Bugge, T. V., Christensen, M. L. & Keiding, K. 2012 Modeling approach to determine cake buildup and compression in a high-shear membrane bioreactor. *J. Membr. Sci.* **409–410**, 335–345.

Le-Clech, P., Chen, V. & Fane, A. G. 2006 Fouling in membrane bioreactors used in wastewater treatment. *J. Membr. Sci.* **284**, 17–53.

Li, X. & Wang, X. 2006 Modelling of membrane fouling in a submerged membrane bioreactor. *J. Membr. Sci.* **278**, 151–161.

Lu, W. M. & Hwang, K. J. 1993 Mechanism of cake formation in constant pressure filtrations. *Sep. Technol.* **3** (3), 122–132.

Meng, F. & Yang, F. 2007 Fouling mechanisms of deflocculated sludge, normal sludge, and bulking sludge in membrane bioreactor. *J. Membr. Sci.* **305**, 48–56.

Ognier, S., Wisniewski, C. & Grasmick, A. 2004 Membrane bioreactor fouling in sub-critical filtration conditions: a local critical flux concept. *J. Membr. Sci.* **229**, 171–177.

Park, P. K., Lee, C. H. & Lee, S. 2006 Permeability of collapsed cakes formed by deposition of fractal aggregates upon membrane filtration. *Environ. Sci. Technol.* **40** (8), 2699–2705.

Picioreanu, C., Kreft, J. U. & Van Loosdrecht, M. C. M. 2004 Particle-based multidimensional multispecies biofilm model. *Appl. Environ. Microbiol.* **70** (5), 3024–3040.

Pradhan, M., Vigneswaran, S., Ben Aim, R. & Kandasamy, J. 2014 Modelling of particle deposition in a submerged membrane microfiltration system. *Desalination* **350**, 14–20.

Shin, J., Kim, K. H., Kim, J. H. & Lee, S. H. 2013 Development of a numerical model for cake layer formation on a membrane. *Desalination* **309**, 213–221.

Van den Broeck, R., Van Dierdonck, J., Caerts, B., Bissona, I., Kregersman, B., Nijskens, P., Dotremont, C., Van Impe, J. F. & Smets, I. Y. 2010 The impact of deflocculation–reflocculation on fouling in membrane bioreactors. *Sep. Purif. Technol.* **71**, 279–284.

Wisniewski, C., Grasmick, A. & Leon Cruz, A. 2000 Critical particle size in membrane bioreactors: case of a denitrifying bacterial suspension. *J. Membr. Sci.* **178** (1–2), 141–150.

Yoon, S. H., Lee, C. H., Kim, K. J. & Fane, A. G. 1999 Three-dimensional simulation of the deposition of multi-dispersed charged particles and prediction of resulting flux during cross-flow microfiltration. *J. Membr. Sci.* **161**, 7–20.

First received 1 September 2014; accepted in revised form 2 February 2015. Available online 17 February 2015